A New Rolling Pressure Model for an Actual Reversing Cold Rolling Strip Mill

M. Heydari Vini
Department of Mechanical Engineering, Mobarakeh branch, Islamic Azad University, Mobarakeh, Isfahan, Iran
E-mail: m.heydarivini@gmail.com

Received: 9 August 2014, Revised: 15 Fabruary 2015, Accepted: 20 April 2015

Abstract: The forging model for cold rolling is one of the rolling models which is used in rolling calculations. In this model, the final rolling pressure is an average value and it is not as accurate for actual and industrial cases. Also, by using forging model, friction hill curves are plotted due to the central point of rolling bite length while frictional stresses intersect at the neutral point of rolling bite. In this study, a new model based on the forging model is presented to determine the rolling pressure during cold rolling process for using in a reversing tandem mill, where this is called "Improved forging model". In the proposed model, the intersection of the frictional forces is the neutral point. Finally, the computing results from this new model coincide well with the precedent investigations.

Keywords: Friction Hill Curve, Pressure Model, Two Stand Reversing Cold Mill

Reference: Heydari Vini, M., "A new rolling pressure model for an actual cold rolling strip mill", Int J of Advanced Design and Manufacturing Technology, Vol. 8/ No. 2, 2015, pp. 73-80.

Biographical notes: M. Heydari Vini received his MSc in mechanical engineering in 2009 and he is currently a PhD student in Mechanical Engineering at IAU University, Science and Research Branch, Tehran, Iran. He is also a faculty member of Islamic Azad University, Mobarakeh branch, Mobarakeh, Isfahan, Iran. He has authored one book and many papers on rolling technology and metal matrix composites. His research interests and activities are in metal forming, rolling technology and metal matrix composites.

1 INTRODUCTION

Cold thin strip can be rolled on a tandem cold mill or a reverse mill where the work rolls are flattened [1]. Fleck et al., [2] conducted the analysis of cold rolling of foil, and Zhang analyzed the rolling of thin foils [3]. Sutcliffe and Rayner developed a model for rolling of thin strip [4]. Matsumoto presented an analysis model of flat cold and temper rolling elastic deformation of thin strip [5]. In other researches, its shape and flatness has been calculated [6], [7]. The analysis of cold rolling process has attracted the attention of a number of researchers. The slab method is one of the best methods which can be applied for analyzing the rolling force and torque. In this method, a slab of infinitesimal thickness is selected perpendicular to the rolling direction at an arbitrary point in the rolling length. First of all, force balance is made on the element by the slab method. From force balance a differential equation in term of the forming stress is formulated. Then, the constants of integration are derived using appropriate boundary conditions.

Starting from the pioneering work of von Karman, some researchers have applied slab method for the analysis of flat cold rolling process [8], [9–12]. In the case of thin strip or foil (thickness below 0.2 mm) rolling, deformation may be considered fairly homogeneous across the thickness of the strip. Hitchcock's formula [13] used by early researchers which is based on the assumption that the work rolls remains rigid and hence because of roll flattening, it cannot be used for foil rolling. Fleck et al., [14] have developed a theory for cold rolling of foil using slab method. In their model, the effect of frictional forces on roll deformation has been neglected. They have not considered strain hardening.

Dixit et al., [15] developed a Finite Element Model of cold flat rolling process. In his model, the effect of strain hardening and friction model is highlighted. Shi et al., [16] have observed a significant difference between the roll torque computed by energy balance method and that computed by taking the moments exerted on the work rolls by the strip. For plasticity problems, some friction models have been used to evaluate applied loads, material flows and deformation, as reviewed by Schley [17]. For dynamic friction force model, Tan has developed a new dynamic friction model and he has successfully applied it to establish solution to the point-strain compression [18].

In the forging model for rolling calculations, friction hill curves are plotted due to the central point of the rolling bite while frictional stresses intersect at the neutral point. In this study, a new model based on the forging model is presented to determine the rolling pressure during cold rolling process. Also, in all mentioned studies, the presented rolling force or rolling pressure models are not applicable in actual cold rolling conditions. In their calculations, many of rolling parameters are not inserted. The forging model for cold rolling process is based on the slab method. By using this model, the computed rolling pressure is very different from an actual rolling process. Many parameters occur during the cold rolling such as work rolls flattening. These problems influence on the rolling pressure.

The new model is a function of some rolling process such as Flattened roll radius, Forward slip of the strip, forward and backward tensile stresses exerted at the ends of strip, static deformation resistance and velocity of strip before and after rolling. Being applicable for actual rolling conditions is the novelty of the presented model in this study. Based on this model, the strip is pressed between the work rolls according to Fig. 1(a). According to Fig. 1 (b), as the strip enters the rolling gap with h_0 thickness, it begins to press and it reaches to h_f thickness. The rolling pressure, increases from the entrance point to the exit point. The maximum amplitude of the rolling pressure is in the neutral point according to Fig. 1 (b).

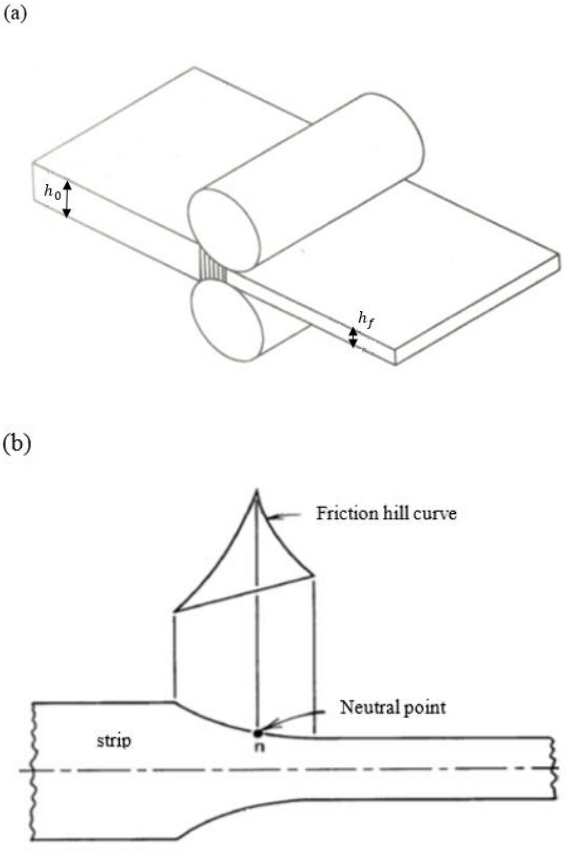

Fig. 1 (a) Compression of strip between two work rolls (b) Friction hill curve along the rolling arc of contact

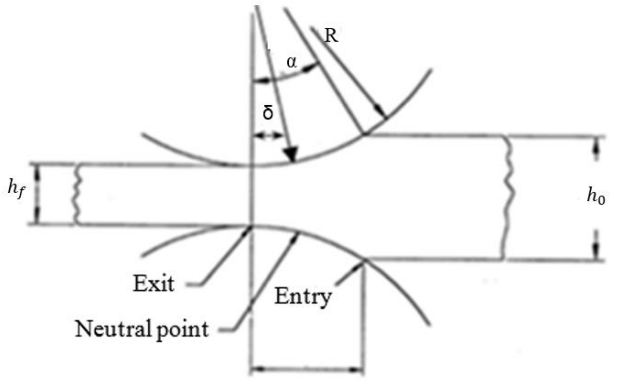

Fig. 2 Roll bite geometry and rolling parameters

As it can be shown in Fig. 2, the roll radius, rolling angles corresponding to the rolling arc of contact and the neutral point are R, α and δ. Finally, based on the forging model, a new model for computing the rolling pressure and load for actual cold rolling conditions has been proposed.

2 MODELIZATION OF THE PROCESS

Fig. 3 shows the rolling of a strip with **h** thickness and **b** width with a plane strain condition. The width of Strip does not change during the rolling process and the plastic deformation is in the **x-y** plane.

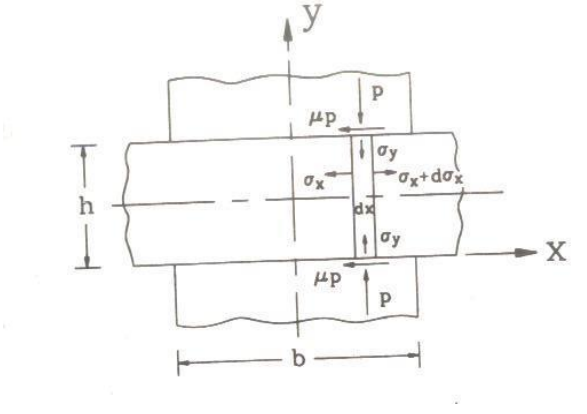

Fig. 3 Stress distribution along the rolling length

The stresses of strip during the rolling are plotted according to Fig. 3, where the equilibrium of the forces along the **x** axis will be:

$$(\sigma_x + d\sigma_x)hw - \sigma_x hw - 2\mu p dx w = 0 \quad (1)$$

Where σ_x is along the **x** axis, **P** and **μ** are rolling pressure and friction coefficient. So, **μp** is the shear stress due to frictional forces. The direction of the shearing forces is toward the inside plane of rolling bite. By simplification Eq. (1), leads to:

$$hd\,\sigma_x - 2\mu p dx = 0 \quad (2)$$

Because of a very low friction coefficient, $\sigma_y = -p$. According to Von Misses plane strain condition:

$$\sigma_1 - \sigma_3 = \sigma_x - \sigma_y = \sigma_x + p = 2k \quad (3)$$

Because the flow friction coefficient **2k** is constant, Eq. (3) becomes:

$$d\sigma_x = -dp \quad (4)$$

By substituting equation (4) into Eq. (2), leads to:

$$\frac{dp}{p} = \frac{-2\mu}{h} dx \quad (5)$$

Solving the Eq. (5), gives:

$$\ln p = \frac{-2\mu}{h} x + c \quad (6)$$

Applying the boundary condition: at $\varphi = 0, p = 2k_f$ into Eq. (6), the amount of **c** becomes:

$$\ln p = \frac{-2\mu}{h} R'\delta + C \rightarrow c = 2k_f \quad (7)$$

Where δ, is the neutral point and R' is the flattened work roll radius. Therefore, the distribution of the rolling pressure from neutral point to exit point can be obtained as:

$$\frac{p}{2k_f} = e^{\frac{2\mu R'(\varphi)}{h}} \quad (8)$$

Eq. (8) is the rolling Pressure over the rolling bite. Thus, the rolling force, is given by:

$$F = \int_0^{\delta} p^+ d\varphi + \int_{\delta}^{\alpha} p^- d\varphi \quad (9)$$

Where h_0 and h_f are thicknesses of strip before and after rolling. p^+ is rolling pressure from entrance point to the neutral point and p^- is output rolling pressure from the neutral point to the exit point.

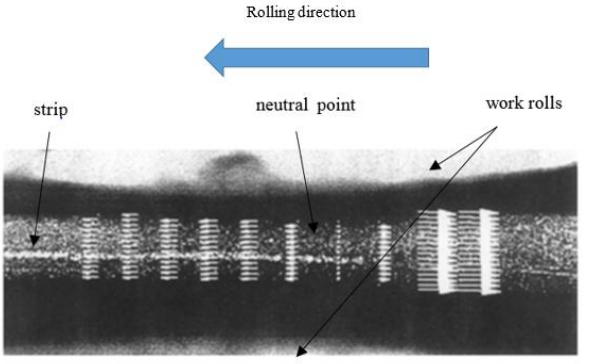

Fig. 4 Vectors of friction forces along the rolling arc of contact [19]

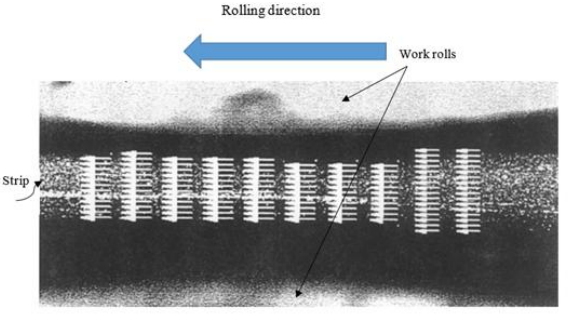

Fig. 5 Speed vectors along the rolling arc of contact [19]

The friction hill or rolling pressure curve is rolling pressure distribution at every point of the rolling bite. This pressure increases from the entrance point and its maximum amplitude is at the neutral point. In the neutral point, the friction forces are in opposite directions (Fig. 4). Fig. 5 shows the speed vectors along the rolling arc of contact. According to Fig. 5, the rolling speed increases from the entrance to exit point. In the neutral point, the difference of speeds of strip and rolls are zero. During an actual or industrial cold rolling process, the exit speed of strip is greater than the peripheral speed of work rolls. This difference is due to the forward slip of rolling process. During the rolling according to Eq. (10), the exit speed of strip is greater than the peripheral speed of work rolls. In Eq. (10), f_s is the forward slip of strip, [20].

$$\mathrm{f}_s = \frac{v_0 - v_r}{v_r} \tag{10}$$

Bland and Ford showed that the forward slip should be computed as a function of cold rolling parameters and strip geometry according to Eq. (11), [20].

$$\mathrm{f}_s = \left(\tan\sqrt{\frac{\zeta}{2}}\mathrm{H_n}\right)^2 \quad \& \quad \frac{h_0}{R'} = \zeta(h_0, R') \tag{11}$$

$$H_n = H_n(\zeta, h_i, h_o, \sigma_b, \sigma_f, k_i, k_o, \mu) \quad \&$$
$$H_1 = \left(\frac{2}{\sqrt{\zeta}}\tan^{-1}\frac{\Phi_1}{\sqrt{\zeta}}\right) = \left(\frac{2}{\sqrt{\zeta}}\tan^{-1}\frac{\frac{\mathrm{h_i}-\mathrm{h_0}}{R'}}{\sqrt{\zeta}}\right) \tag{12}$$

In Eq. (12), ζ and H_n are two functions. Also, $\mathrm{k_i}$ and $\mathrm{k_0}$ are resistances to the deformation of strip before and after the plastic deformation of rolling process. The other essential parameters are [20]:

$$H_n = \left(\frac{h_1}{2}\right) - (2\mu^{-1})\ln\left\{\left(\frac{h_i}{h_0}\right)\frac{\left(1-\frac{\sigma_f}{k_0}\right)}{\left(1-\frac{\sigma_b}{k_i}\right)}\right\} \tag{13}$$

Finally, the friction coefficient during the cold rolling becomes [20]:

$$\mu = \frac{\ln\left(\frac{\left(\frac{\mathrm{h_i}}{\mathrm{h_0}}\left(1-\frac{\sigma_f}{k_0}\right)\right)}{\mathrm{H_1}-\left(\left(\frac{4}{\zeta}\right)\tan^{-1}\sqrt{\mathrm{f_s}}\right)}\right)}{H_1-\left(\frac{4}{\sqrt{\zeta}}\right)\tan^{-1}\sqrt{f_s}} \tag{14}$$

According to Akulund's model, the roll flattened radius is [21]:

$$R' = R\left(1 + \frac{C}{\Delta h}.\frac{F}{W}\right) \tag{15}$$

From ref. [21], the amount **C** for steel rolls is 0.22×10^{-4}. $\mathrm{t_b}$ and $\mathrm{t_f}$ are backward and forward tensile stresses. The rolling pressures with backward and forward tensile stresses can be derived as:

$$p^+ = 2k_f\left(1 - \frac{t_f}{2k_f}\right)e^{\frac{2\mu R'(\varphi)}{h_f + R'\varphi^2}}$$
$$p^- = 2k_0\left(1 - \frac{t_b}{2k_b}\right)e^{\frac{2\mu R'(\alpha-\varphi)}{h_f + R'\varphi^2}} \tag{16}$$

By equalizing the rolling pressures from Eq. (16) at both sides of the rolling bite, the neutral point will be determined as:

$$\delta = \left(\frac{1}{2\sqrt{\frac{R'}{h_f}}\tan^{-1}\sqrt{\frac{R'}{h_f}}}\right)\left(\frac{1}{2\mu}\ln\frac{2k_0\left(1-\frac{t_b}{2k_o}\right)}{2k_f\left(1-\frac{t_f}{2k_1}\right)} + \frac{\mu H_o}{2}\right) \tag{17}$$

By increasing the number of points, the accuracy of the plotted friction hill curves increases. In this study for validating the new rolling pressure model, the information used, are from an industrial cold rolling process. They have been obtained from a rolling

program in two stand reversing cold mill which are listed in tables 1 and 2.

Table 1 Rolling process in two stand reversing cold mill [20]

Rolling process						
Pass	stand	Initial thickness (mm)	Final thickness (mm)	Backward tensile stress	Forward ensile stress	friction coefficient (μ)
				Mpa	Mpa	
1	1	2	1.3	10.3	185.4	0.05
	2	1.3	0.86	185.4	108.1	0.06
2	2	0.86	0.56	108.1	195.7	0.03
	1	0.56	0.4	195.7	164.8	0.05
3	1	0.4	0.31	164.8	206	0.04
	2	0.31	0.25	206.	65.1	0.03

Table 2 Strip properties in two stand reversing cold mill [20]

Strip properties	
St1008	
Poisson's ratio	0.29
Modulus of elasticity	200 Gpa
Yield strength	280 Mpa
Plastic stress-strain relation	$\sigma_p = 658\varepsilon_p^{0.24}$
Density	$7.782\ \frac{ton}{m^3}$
Poisson's ratio	0.29
Modulus of elasticity	200 Gpa

3 RESULTS AND DISCUSSION

Fig. 6 shows the two stand reversing cold mill system. According to Fig. 6, there are 3 passes with 2 Steps in each rolling pass. First of all, a coil is fed into the payoff reel and it was passed among two stands and its end was clamped at the delivery reel. The first cycle does among the payoff and the delivery reels and the second will be done on the opposite direction between the delivery and input reels. Finally the third will be done in the opposite direction between the same reels [20]. In Fig. 7, friction hill curves are plotted according to the table 1 from neutral point to the exit point. In Fig. 8, they are plotted along the total rolling arc of contact by the present rolling pressure model.

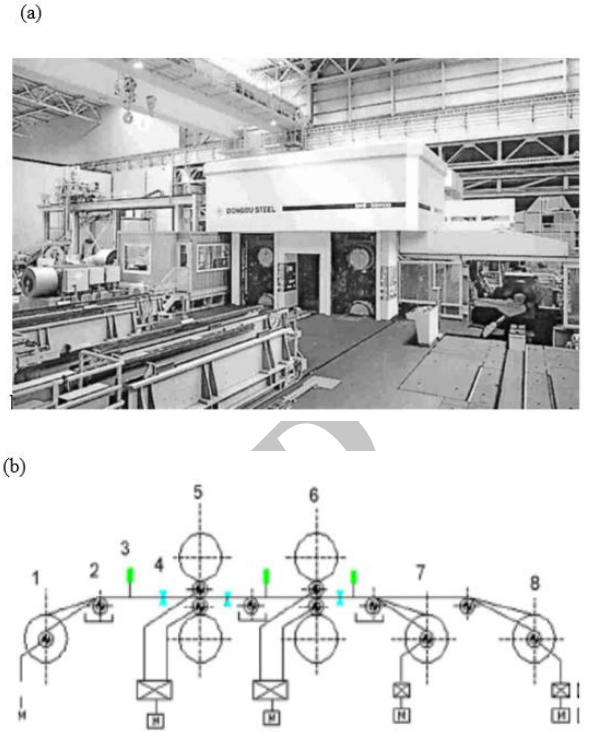

Fig. 6 (a) Two stand reversing cold mill (b) Stand tandem cold strip mill process (1) Delivery reel, (2) Tension meter, (3) Laser speedometer, (4) Thickness gauge, (5) Stand #2, (6) Stand #1, (7) Input reel and (8) Pay off reel

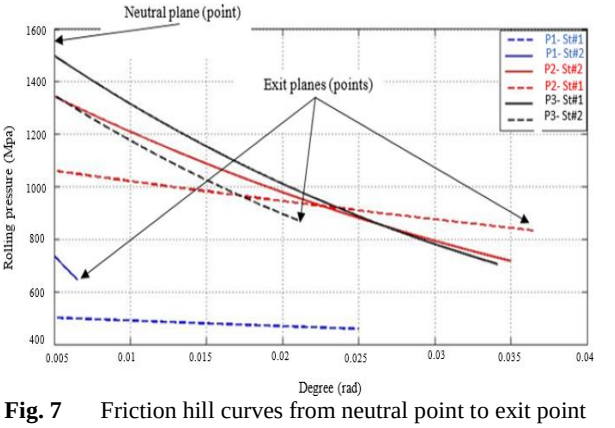

Fig. 7 Friction hill curves from neutral point to exit point according to Table 1

Fig. 4 shows the friction hill curves based on the new model. According to Fig. 4, increasing the rolling passes, increases the rolling pressure and work roll flattening. Figs. 7 and 8, show the accuracy of the new model. This is an applicable model to determine the rolling pressure during the reversing cold rolling process in actual conditions.

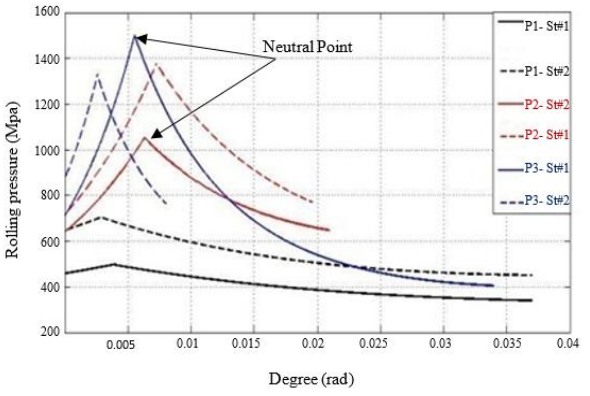

Fig. 8 Friction hill curves for cold rolling process according to Table 1

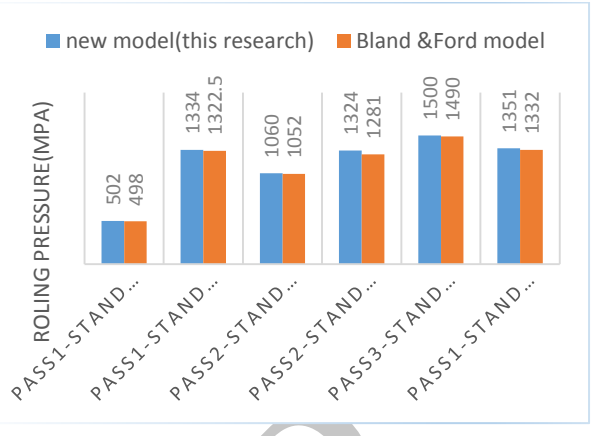

Fig. 9 Comparison of maximum cold rolling pressure obtained from Bland & Ford model with the new model

In Fig. 9, the maximum rolling pressure obtained from Bland and Ford model is compared with the present pressure model based on tables 1, 2, where they coincide well together. According to Fig. 10, forward tensile exerted on the ends of strip, reduces the rolling pressure from the neutral to the exit point and it also moves the neutral position toward entrance direction, where this decreasing amount is based on Eq. (18).

$$P^{+}{}_{f} = 2k_f(1 - \frac{t_f}{2k_f}) \tag{18}$$

Increasing the number of rolling passes, increases the work roll flattening and the rolling load. Increasing rate of rolling load when the rolls are rigid, are less than when the rolls begin to flat. Because of the roll flattening, there is a severe increase in the rolling forces in final passes of rolling process. As it demonstrated in Fig. 10, the forward tensile stress exerted at the ends of strip decreases the pressure at output point of rolling bite. Also it decreases the work hardening of the strip. According to Fig. 11, backward tensile stress exerted at the ends of strip moves the position of the neutral point toward the exit side and it also decreases the rolling pressure at the entrance point of the rolling bite, where this decreasing amount is based on Eq. (19). Because of higher frictional surfaces, not only roll flattening increases the amount of rolls power, but also it increases backward slip at the entrance point [22].

$$P^{-}{}_{b} = 2k_b(1 - \frac{t_b}{2k_b}) \tag{19}$$

In Fig. 12, the effect of tensile stresses on the rolling pressure and on the residual stresses of strip is considerable. In Fig. 12, the new neutral point is the intersection of blue and red curves which is about 0.008 radian of rolling bite angle.

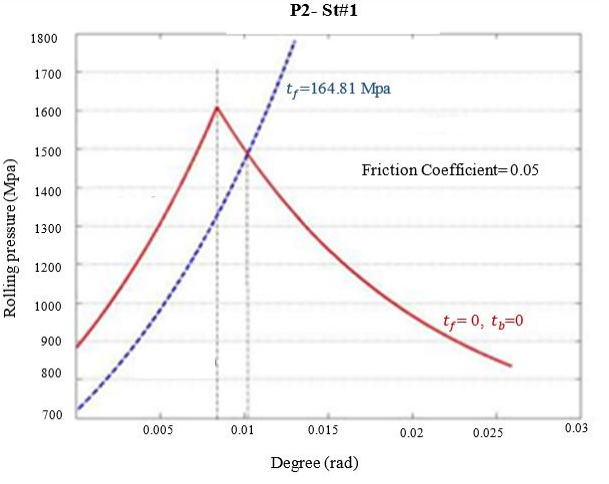

Fig. 10 Effect of forward tensile stress on the rolling pressure

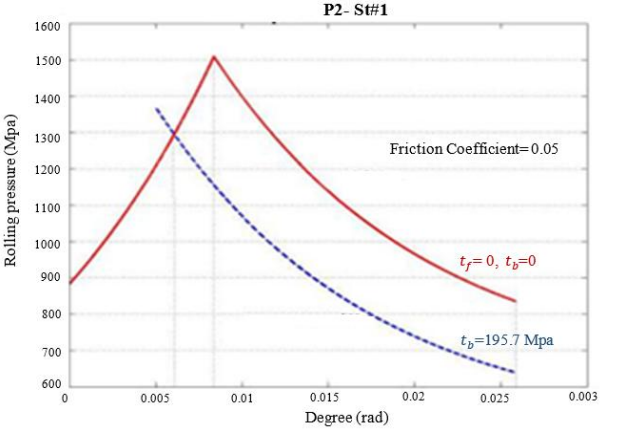

Fig. 11 Effect of backward tensile stress on the rolling pressure

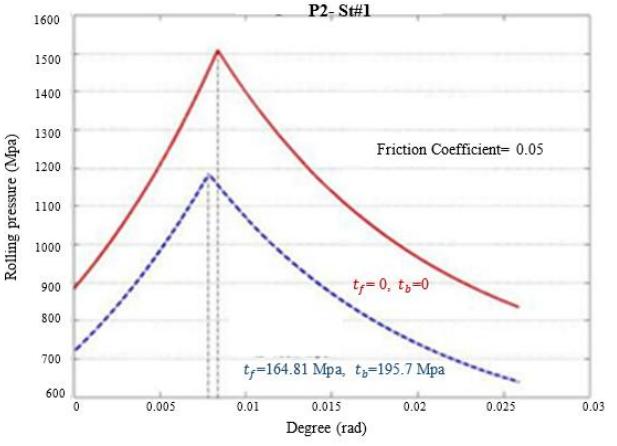

Fig. 12 Effect of applied forward and backward tensile stresses on the rolling pressure

Figs. 7-12 demonstrate the accuracy of new model in compliance with Bland and Ford model. In the new model, the origin of coordinate along the horizontal axis is the exit point.

4 CONCLUSION

a. The most work hardening and residual stresses are in the first pass and there is a good compliance with pass1-stand#1 with other researcher's results such as Larke and Rowe [23].

b. According to Fig. 11, there is a good compliance with Bland & Ford and the presented model. The proposed model can be used for industrial reversing cold rolling processes.

c. Tensile stresses applied to the ends of strip decrease the rolling pressure.

d. Backward tensile stress exerting at the end side of strip, moves the position of the neutral point toward the exit side. Also, it decreases rolling pressure at the entrance point of rolling bite.

e. Forward tensile stress exerting at the end side of strip moves the position of the neutral point toward the entry side and also, it decreases the rolling pressure at the exit point of rolling bite.

5 NOMENCLATURE AND SUBSCRIPTS

σ	Normal stress [Mpa]
μ	Friction coefficient
p	Rolling pressure [Mpa]
k	Shear strength of strip [Mpa]
h	Thickness of strip [mm]
h_0	Initial thickness of strip [mm]
h_f	Final thickness of strip [mm]
R	Work roll radius [mm]
R'	Flattened roll radius [mm]
α	Rolling arc angle [radian]
δ	Neutral point angle [radian]
Φ	Rolling bite angle [radian]
k_f	The deformation resistance of strip at the exit point [Mpa]
v_r	Peripheral speed of the work rolls [mm/sec]
v_0	Exit speed of strip [mm/sec]
k_i , k_0	Resistances to the deformation of strip before and after rolling [Mpa]
f_s	Forward slip of the strip [Mpa]
t_b	Backward tensile stress [Mpa]
t_f	Forward tensile stress [Mpa]
W	Width of strip [mm]
σ_y	Yield strength of the strip [Mpa]

ACKNOWLEDGMENTS

Support of R&D of Mobarakeh steel company is appreciated.

REFREENCES

[1] Montmitonnet, P., E. Massoni, M. Vacance, G. Sola, P. Gratacos, "Modelling for geometrical control in cold and hot rolling", Iron making Steelmaking 20, 1993, pp. 254-260.

[2] Fleck, N. A., Johnson, K. L., Mear, M. E., and Zhang, L. C., "Cold rolling of foil", Proc. Inst. Mech. Eng. Part B: J. Eng. Manuf. 206, 1992, pp. 119-131.

[3] Zhang, L. C., "On the mechanism of cold rolling thin foil", J. Mach. Tools Manuf. 35, 1995, pp. 363-372.

[4] Sutcliffe, M. P. F., Rayner, P. J., "Experimental measurements of load and strip profile in thin strip rolling", Int. J. Mech. Sci. 40, 1998, pp. 887-899.

[5] Matsumoto, H., "Elastic-plastic theory of cold and temper rolling", Proceedings of the Eighth International Conference on Technol. Plast., Verona, Italy, October 9–13, 2005, pp. 521-522.

[6] Jiang, Z. Y., Tieu, A. K., Zhang, X. M., Lu, C., and Sun, W. H., "Finite element simulation of cold

rolling of thin strip", J. Mater. Proc. Technol. Vol. 140, 2003, pp. 542-547.
[7] Jiang, Z. Y., Tieu, A. K., "Elastic-plastic finite element method simulation of thin strip with tension in cold rolling", J. Mater. Proc. Technol. Vol. 130-131, 2002, pp. 511–515.
[8] Von Karman, T., "On the theory of rolling", Z. Angew. Math. Mech, Vol. 5, 1925, pp. 139-141.
[9] Orowan, E., "The calculation of roll pressure in hot and cold flat rolling", Proc. Inst. Mech. Eng. 150, 1943, pp. 140–167, J. Eng. Manuf. 206, 1992, pp. 119-131.
[10] Bland, D. R., Ford, H., "The calculation of rolls force and torque in cold strip rolling with tensions", Proc. Inst. Mech. Eng., Vol. 159, 1948, pp. 144-153.
[11] Bland, D. R., Sims, R. B., "A note on the theory of rolling with tensions", Proc. Inst. Mech. Eng., Vol. 167, 1953, pp. 371–374
[12] Alexander, J. M., "On the theory of rolling", Proc. R. Soc. Lond. A 326, 1972, pp. 535–563.
[13] Hitchcock, J. H., "Roll Neck Bearings", Report of ASME Research Committee, 1935.
[14] Fleck, N. A., Johnson, K. L., Mear, M. E., Jhang, L. C., "Cold rolling of foil", Proc. Inst. Mech. Eng. 206, 1992, pp. 119–131.
[15] Dixit, U. S., Dixit, P. M., "A finite element analysis of flat rolling and application of fuzzy set theory", Int. J. Mach. Tools Manuf. 36, 1996, pp. 947–952.
[16] Jingyu Shi, D. L. S., McElwain, Langlands, T. A. M., "A comparison of methods to estimate the roll torque in thin strip rolling", Int. J. Mech. Sci. 43, 2001, pp. 611–630.
[17] Schey, J. A., "Tribology in Metalworking Friction, Lubrication and Wear", American Society of Metals, Metals Park, OH, 1983, pp. 27–130.
[18] Tan, X., "Friction of plasticity: application of the dynamic friction model", Proceedings of the Institution of Mechanical Engineers Part J. J. Eng. Tribol. 221, 2007, pp. 115–131.
[19] Li, E. B. "Application of digital image correlation technique to dynamic measurement of the velocity field in the deformation zone in cold rolling", optics and laser in engineering 39, 2003, pp. 479-488.
[20] Heydari Vini, M., Ebrahimi, H., Ziaeimoghadam, H. R., and Jafarian, M., "A new approach to determine the friction hill curves ,rolling load and analysis of permanent failure of work rolls in an actual cold rolling", International Conference on Materials Heat Treatment (ICMH 2012), Islamic Azad University, Majlesi Branch, May 30-31, 2012, Isfahan, Iran.
[21] Moshksari, M., "Fundamentals of rolling", 2nd ed., Shiraz University, 2005, Chaps. 5, 6, 8.
[22] Kumar, A., Samarasekera, I. V., and Hawbolt, E. B., "Roll-bite deformation during the hot rolling of steel strip", Journal of Materials Processing Technology, Vol. 30, 1992, pp. 91–114.
[23] LARKE, E. C., "The rolling of strip, sheets and plate", science paperback edition, London, 1967, pp. 71-126.